Diagnostics of a converging strong shock wave generated by underwater explosion of spherical wire array

O. Antonov, S. Efimov, V. Tz. Gurovich, D. Yanuka, D. Shafer, and Ya. E. Krasik
Physics Department, Technion, Haifa 32000, Israel

(Received 10 February 2014; accepted 2 June 2014; published online 12 June 2014)

The results of experimental studies of the convergence of shock waves (SWs) generated by the underwater electrical explosion of a spherical wire array supplied by a current pulse with an amplitude ~300 kA and rise time ~1.1 μs are reported. In the experiments, the power and spectrum of the light emission from an optical fiber, the explosion of a copper tube, and the time-dependent resistance of a resistor placed in the equatorial plane of the spherical wire array were measured. A comparison of the experimental data with the results of numerical simulations of SW convergence shows that the SW keeps its uniformity along the major part of the convergence towards the implosion origin. © *2014 AIP Publishing LLC*. [http://dx.doi.org/10.1063/1.4883187]

I. INTRODUCTION

Various interesting physical phenomena related to warm dense matter (WDM) have attracted the interest of many researchers in the last decades.[1–3] Different dynamic loading facilities, such as multi-stage light gas guns,[4] Z-pinch,[5] powerful lasers,[6,7] and intense heavy ion beams,[8] with a stored energy in the range of 10^5–10^9 J, are required to generate extreme states of matter[9] characterized by a pressure $P \geq 10^{11}$ Pa during a short (in the range 10^{-9}–10^{-6} s) time duration. Recent research[10–12] showed that by using a pulsed power generator with stored energy of only a few kJ as a current source for the underwater electrical explosion of a wire array, one can generate WDM with $P \leq 6 \times 10^{12}$ Pa. This method exploits the converging strong shock waves (SWs) generated by the underwater electrical explosion of either a cylindrical or a spherical wire array. The parameters of the water (pressure, temperature, and density) in the vicinity of either the convergence axis, in the case of a cylindrical SW, or the origin of the convergence, in the case of a spherical SW, were calculated using one-dimensional hydrodynamic (1D-HD) simulations coupled with the experimentally measured energy deposited into the wires and the equation of states for water.[13] The results of these simulations were considered acceptable in terms of the fitting between the simulated energy, which is transferred to the water flow and should be smaller than 12% of the experimentally measured energy deposited into the exploding wires,[14,15] and the experimentally measured and simulated time-of-flight (TOF) of the converging SW. In addition, these simulations assume longitudinal and azimuthal uniformity of the converging SW, which in the case of a 5 mm in radius cylindrical wire array explosion was obtained experimentally down to a radius of convergence $r \approx 100$ μm, resulting in a convergence ratio of at least 50. Here, let us note that two-dimensional hydrodynamic (2D-HD) simulations[16] showed that non-uniformity of the cylindrical converging SW should be self-repaired,[17] or, in the worst case, the pressure in the vicinity of the implosion calculated by 1D-HD would be decreased by a factor of 2. In spite of the long history of this research, the issue where the converging spherical SW is unstable, which is in fact a 3D problem, still requires more investigation, in particular, in the case of an SW converging in water.

In this paper, we present the results of recent experiments in which additional diagnostics were used for estimating and measuring the pressure in the vicinity of the implosion of the spherical SW. The data obtained indicate strongly that the SW generated by underwater electrical explosion of a spherical wire array retains it uniformity during the main part of its convergence.

II. EXPERIMENTAL SETUP AND RESULTS

To explode the spherical wire arrays having a diameter of 40 mm, 30 mm, 25 mm, and 20 mm and consisting of 40 copper wires each with a diameter of 100 μm, a microsecond timescale high-current generator[12] (stored energy of ~3.6 kJ, current amplitude and rise time of ~300 kA and ~1.1 μs, respectively) was used (see Fig. 1). The typical discharge voltage φ_d and current I_d waveforms, measured by a Tektronix voltage divider and corrected on an inductive voltage component LdI_d/dt (here L is the load inductance) and self-integrated Rogowski coils, respectively, and the calculated power $P(t) = [\varphi_d(t) - LdI_d(t)/dt]I_d(t)$ and energy $W = \int_0^t P(t)dt$ deposition into the wires are shown in Fig. 2. One can see that the discharge is aperiodic, which is typical for underwater electrical explosion of wires[18,19] characterized by fast phase transitions of exploding wires: solid state–liquid–vapor–plasma. The main energy deposition to the exploding wires occurs during the formation of plasma that is rather low-temperature (several eV) and low-ionized, i.e., the resistance of each exploded wire increases up to 8 Ω. This phase begins at the time when one obtains a fast decrease in the discharge current. One can see that in the present experiment ~80% of the stored energy is delivered to the exploding wire array during ~500 ns. The results of earlier research,[14,15] which showed that the efficiency of the transfer of the energy deposited into the exploded wire to the water flow is ~24%, allow one to estimate that ~12% of this deposited energy is transferred to the converging water flow, i.e., ~350 J of ~3000 J of deposited energy.

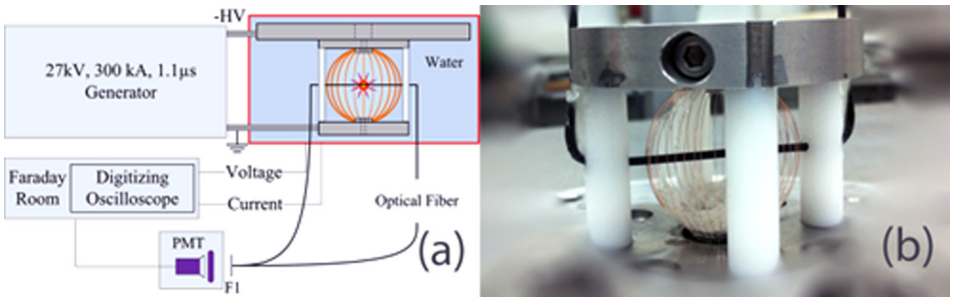

FIG. 1. (a) Experimental setup; (b) External view of the 40 mm diameter wire array composed of 40 Cu wires each 100 μm in diameter.

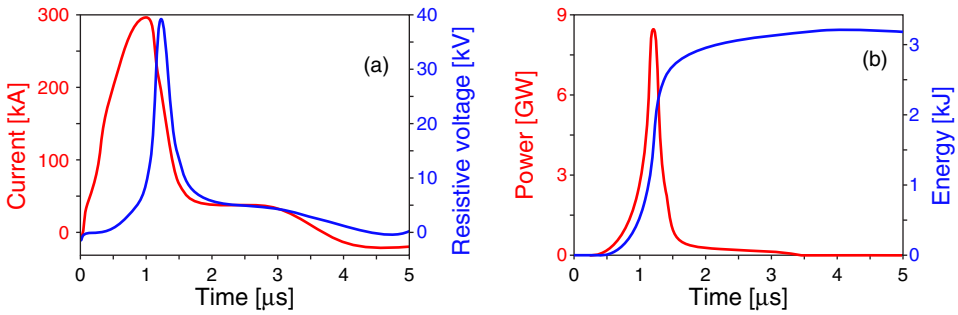

FIG. 2. Waveforms of (a) discharged current and the resistive voltage and (b) deposited power and energy. The wire array 40 mm in diameter, consisting of 40 Cu wires, each 100 μm in diameter.

Because there is no optical access (contrary to the case of the explosion of a cylindrical wire array[11]), the diagnostics of a spherically converging SW is rather problematic. Indeed, only the last few tens of microns of spherical SW propagation in the vicinity of the converging origin were obtained by detecting intense light emission from that location, and these data were used as the TOF for comparison with the results of the 1D-HD simulations.[12,20]

In the present experiments, we studied the dynamics of the convergence of the spherical SW using measurements of the change in the intensity of the CW laser beam ($\lambda = 532$ nm, 30 mW) guided by a lens to the input of the optical fiber. The fiber has a core diameter of 0.2 mm and it was covered by a non-transparent thin (0.25 μm) dielectric tube. The fiber was placed in the equatorial plane of the spherical wire array (see Fig. 1(b)) and the intensity of the laser beam was monitored using an FDS-100 Thorlabs photodiode (~10 ns time resolution) coupled with the output end of the fiber. Typical waveforms of the laser intensity together with the discharge current pulse are shown in Fig. 3. First,

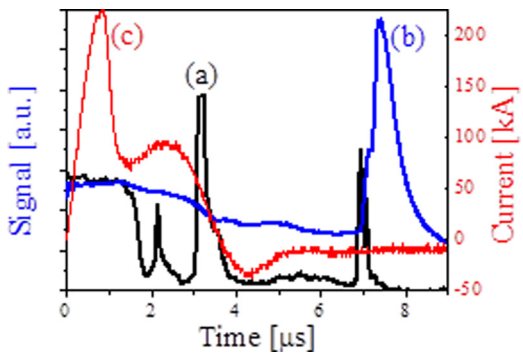

FIG. 3. (a) Intensity of the CW laser emission as detected by photodiode using typical spherical wire array. (b) Intensity of the CW laser emission as detected by photodiode using modified spherical wire array. (c) Discharge current through the spherical wire array during the explosion.

when the fiber was placed in the original wire array having a diameter of 30 mm, we obtained [see waveform (a) in Fig. 3] a drastic decrease in the laser intensity starting at time delay $\tau_d \sim 0.45$ μs with respect to the beginning of the wires' explosion (i.e., with respect to the beginning of the explosion accompanied by the generation of SSWs and at the time when a fast decrease in the discharge current is obtained[18,19]), followed by a rather sharp and short (~100 ns time duration) recovery of the light intensity (first peak). The decrease in the light intensity can be explained by the fiber's decreased transparency (change of density and, respectively, refraction index) because of its interaction with SWs generated by the explosion of adjacent wires. Indeed, the distance between the wires in the equatorial plane was ~2.6 mm, which results in a time of ~0.4 μs being needed for SWs propagating with a Mach number $M \approx 1.3$ (Ref. 21) to overlap each other. The recovery of the light intensity (first peak) could be related to triboluminescence phenomena caused by the interaction of these two SWs and the possible partial damage to the fiber. The second, more intense, peak in the light intensity having a duration of ~0.5 μs at Full Width Half Maximum (FWHM) obtained with $\tau_d \sim 2.1$ μs is related to the interaction of the fiber with the expanded dense plasma channel generated by the wires explosion, whose average expansion velocity is $\sim 5 \times 10^4$ cm/s. Finally, the third peak in light intensity, which appears at a time delay consistent with the TOF data, is caused by the SW's implosion and the total destruction (explosion) of the fiber at that location. In order to avoid the interaction of the fiber with SWs generated by the explosion of adjacent wires and by expanding dense plasma channels, the azimuthal distance between these wires was increased up to ~5 mm. In this case, the waveform of the light intensity of the laser beam [see curve (b) in Fig. 2] indeed showed the absence of the first and second peaks and an approximately linear decrease with a sharp peak at the time of the SW implosion. At the present, we do not

know what phenomena are responsible for this almost linear decrease in the laser light intensity. One can suppose that this decrease is related to the change in the ratio between the core and cladding diameters because of the different compressibility of these materials, resulting in an increase in the losses of the propagating laser beam. In addition, the change in the refraction index because of the increase in the fiber density caused by the converging SSW and following water flow can be a reason for the scattering of the laser light, increasing its losses. Thus, because of the unknown change in the ratio between the core and cladding diameters and/or of the refraction index on pressure, the obtained dependence of the attenuation of the laser light intensity was not used to reconstruct the propagation of the SW. However, the attenuation of laser light intensity just prior to the appearance of the intense light emission (a sharp peak at the time of the SW implosion) was used to estimate the power of this emission, ~300 mW using the known spectral sensitivity of the calibrated diode and known intensity of the laser emission.

Further, using the same optical fiber, placed at the equatorial plane, spectroscopic measurements of this emission were conducted using imaging spectrometer (150 grooves/mm, spectral resolution ~4 Å/pixel) coupled with a 4QuikE intensified camera at its output. The obtained radiation spectrum in the range 480–580 nm can be characterized as continuous. Using the known emission from the Oriel QTH200 lamp and assuming Planckian radiation, the best fit for the obtained spectrum occurs when the temperature is ~3300 K (see Fig. 4). For comparison, simulated Planckian spectra for temperatures of 3200 K and 3400 K are shown in Fig. 4, as well. Now, using the data for the power of the emission (~300 mW) and temperature (~3300 K) of the fiber one can estimate the radius of the fiber surface that should emit this radiation. A black body with a temperature of 3300 K emits a power density of 6.7 W/mm^2, an emission power that meets the conditions of a sphere with a radius of $r = 60\,\mu$m. On the other hand, using the results of the 1D-HD simulations in which spherical symmetry of the converging SW was assumed, one obtains the convergence radius $r = 100\,\mu$m as that at which the temperature at the SW front reaches 3300 K. Here, let us note that the simulations were conducted for SW convergence in water, and therefore, they did not account for partial reflection of the SW from the fiber. Thus, one can state that there is satisfactory agreement between the results of simulations and experiments indicating uniformity of the converging SW. It is understood that this analysis can be considered to be approximate, because it contains several not yet proved assumptions, such as perfect Planckian emissivity, negligible power of radiation in the IR and UV range of the spectrum, and a constant attenuation coefficient.

In our recent experiments,[20] different (copper, aluminum, carbon) small ($\leq$0.8 mm) diameters rods were placed in the equatorial plane of the wire array. As a result of the implosion of the generated converging SW, the destruction of the rods was obtained exactly in the center of the sphere. In the present research, a deformation of a thin copper tube (outer radius $r \approx 0.05$ cm, wall thickness $d \approx 0.01$ cm), which was placed in equatorial plane of the wire array (array diameter of 30 mm), was used to estimate the parameters of the SW approaching this tube. An external view of the damage to the copper tube, which was obtained more or less symmetrically along the tube axis, while the damaged part of the tube was located with rather high accuracy in the vicinity of the implosion, is shown in Fig. 5. One can see that this damage seems to have been caused by an explosion of the tube produced by the pressure generated inside the tube by compressed and heated gas. That is, close to the origin of the implosion and the damaged part of the tube one obtains an increase in the radius of the tube up to 0.07 cm. In addition, it was found that at a small distance, ≈0.05 cm, from the damaged part the tube was compressed and its radius did not exceed ≈0.035 cm. Thus, one can suppose that this compressed part of the tube almost closed the internal diameter, i.e., "cut off" the central part of the tube where generated high pressure leads to explosion of the tube.

Let us estimate the energy that the converging SW transferred to the tube. A qualitative diagram of the SSWs propagating in water and interacting with the tube, reflected SSWs, and SSWs propagating in the tube wall are shown in Fig. 6, together with the directions of the water and tube material flows.

The pressure P_1 and density $\rho_1 = 1/V_1$ of water behind the front of the SW are related to each other by the known polytropic equation of the EOS of water $P_1 - P_0 = A[\delta_1^a - 1]$, where $A \approx 3 \times 10^8$Pa, $\delta = \rho_1/\rho_0 = V_0/V_1$ is the water compression, $\rho_0 = 1/V_0$ and $\rho_1 = 1/V_1$, V_0 and V_1 are the density

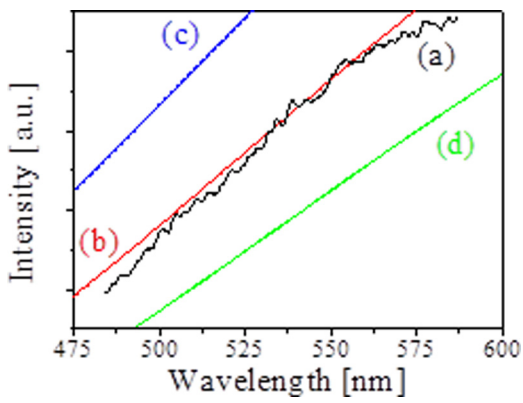

FIG. 4. (a) Experimental spectrum of self-light emission from the fiber. (b-d) Simulated emission spectrum of a black body with temperature of 3300 K (b), 3400 K (c), and 3200 K (d).

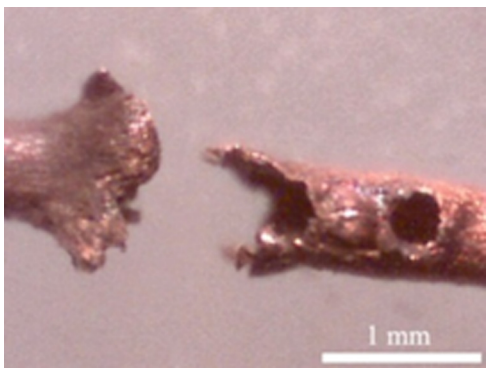

FIG. 5. External view of a Cu tube after the experiment with the explosion of a 30 mm diameter Cu wire array.

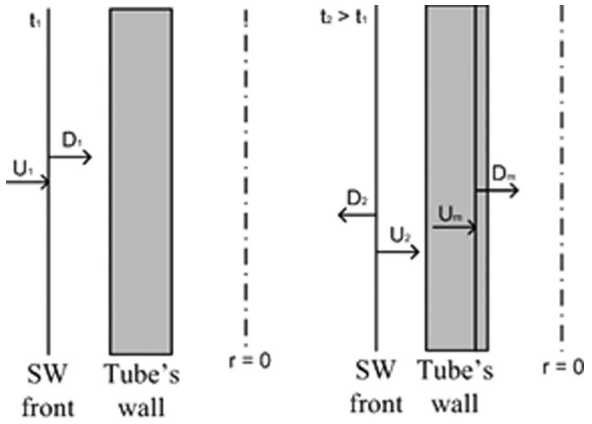

FIG. 6. A qualitative diagram of the SSWs propagating in water and interacting with the tube, reflected SSWs, and SSWs propagating in the tube wall together with the directions of the water and tube material flows.

and unit volumes of water at normal conditions and behind the front of the SW, respectively, and $a = 7.15$. The velocity U_1 of the water flow behind the front of the SW propagating with velocity D_1 can be determined as

$$D_1 = V_0\sqrt{(P_1 - P_0)/(V_0 - V_1)};$$
$$U_1 = \sqrt{(P_1 - P_0)(V_0 - V_1)}. \tag{1}$$

After the reflection of the SW from the wall of the tube, one obtains the formation of the second SW propagating with velocity D_2 in the opposite direction with respect to the primary converging SW. In order to determine the parameters of the water D_2, U_2, and $P_2(\rho_2 = 1/V_2)$ behind the second SW, one has to use mass and momentum conservation laws in the coordinate system related to the second SW, taking into account that in this system the velocity D_2 is directed opposite to the velocity U_1, but velocities U_2 and U_1 have the same directions,

$$U_2 + D_2 = V_2\sqrt{(P_2 - P_1)/(V_1 - V_2)};$$
$$U_1 - U_2 = \sqrt{(P_2 - P_1)(V_1 - V_2)}. \tag{2}$$

Now let us consider the parameters of the SW that is transferred to the tube. At the outer surface of the tube, the pressure in the water $P_2(V_2)$ is equal to the pressure inside the tube material $P_2(V_2) = P_m(V_m)$. The EOS for copper can be described by the polytropic equation[22] $P_m - P_{m0} = B[\delta_m^b - 1]$,where $B \approx 2.5 \times 10^{10}$ Pa, $b = 4$, and $\delta_m = (\rho_m/\rho_{m0})$ is the compression of the copper, P_{m0} and ρ_{m0} are the pressure and density of copper at normal pressure P_m, and ρ_m is the density of copper behind the front of the SW. The velocity D_m of the front of the SW propagation in copper and the velocity U_m of the copper material behind the SW front are determined as

$$D_m = V_{m0}\sqrt{(P_{m1} - P_{m0})/V_{m0} - V_{m1}};$$
$$U_m = \sqrt{(P_{m1} - P_{m0})(V_{m0} - V_{m1})}. \tag{3}$$

Now, taking into account that at the tube-water boundary, $U_2 = U_m$, one can determine the parameters V_2, V_m, D_2, and U_2 using the system of Eqs. (2) and (3) for known parameters of P_1 and V_1. The parameters of the SW in the copper tube allow one to estimate the energy that is transferred to the tube inner wall when the SW reaches this location. The potential and kinetic energy of the unit of mass are determined as[22]

$$\varepsilon_p \approx \frac{B}{\rho_{m0}}\left\{\frac{1}{b-1}\left[\delta_m^{b-1} - 1\right] - \left[1 - \delta_m^{-1}\right]\right\}, \quad \varepsilon_c = U_m^2/2. \tag{4}$$

According to experimental observation, the length of the damaged part of the tube is $L \sim r$ and the mass of this part is $M \approx 2\pi\rho_{m0} rLd$. Thus, the total energy that is deposited into this part of the tube is $E \approx M(\varepsilon_p + \varepsilon_c)$. The implosion of this part toward the axis leads to the formation of the excess pressure of the compressed and heated gas that causes this part of the tube to explode.

The results of the 1D-HD simulations showed that $P_1 \approx 10^{10}$Pa is reached when the converging SW generated by the explosion of a 30 mm wire array reaches the tube's outer boundary at $r \approx 0.05$ cm. Using Eq. (1) and the polytropic EOS of water, one obtains values of $D_1 \approx 5.3 \times 10^3$m/s, $U_1 \approx 2.14 \times 10^3$m/s, and $\delta_1 \approx 1.67$. Now, using Eqs. (2) and (3), one can calculate that the pressure at the water-tube boundary reaches $P_2 = P_m \approx 3.3 \times 10^{10}$Pa, the velocity of the front of the SW propagating in the copper, $D_m \approx 4.4 \times 10^3$ m/s, the velocity of the copper behind this front, $U_m \approx 828$ m/s, and the copper compression, $\delta_m \approx 1.23$. These parameters result in the kinetic and potential energy of the copper wall being $E_c \approx 1.1$ J and $E_P \approx 0.88$ J, respectively, at the time when the SW propagating in the copper reaches its inner boundary.

The destruction of the copper tube occurs in the mode of plastic flow and requires energy per unit of mass $e \approx \sigma_{pl}\varepsilon/\rho_{m0}$ (see, Ref. 23), where $\sigma_{pl} \approx 2 \times 10^9$ Pa is the stress tension of plastic flow for copper and $\varepsilon \approx 0.1$ is the relative strain. Thus, in the case of the explosion of the copper tube, one requires energy of at least $E_{pl} \approx eM$. This energy is transferred to the tube by the converging SW and the water flow that accompanies the SW. Let us calculate that $E = E_{pl} \approx 0.07$ J for the mass $M \approx 3 \times 10^{-6}$ kg of the tube that was destroyed when the SW, propagating inside the copper tube, reached it inner boundary. One can see that this value of energy is significantly smaller than the energy that was estimated above.

When the SW reaches the inner boundary of the copper tube, a fast decrease in the pressure is realized in the copper, accompanied by sharp acceleration, heating, and evaporation of the surface material of the tube.[23] The process that requires the largest energy density is evaporation, which for copper is $\lambda \approx 48.2 \times 10^5$ J/kg. If one considers that all the energy stored in the copper wall will be transferred to this process, in this case the mass of the vapor will be $M_i \approx (E_c + E_p)/\lambda \approx 4 \times 10^{-7}$kg, which is approximately 10 times smaller than the total mass (3×10^{-6} kg) of the damaged part of the tube. This process leads to the density of copper atoms in the tube cavity being up to $n_{Cu} \approx 10^{28}$m^{-3} and a vapor pressure of $P_{0cu} \approx 4.6 \times 10^8$Pa, assuming that

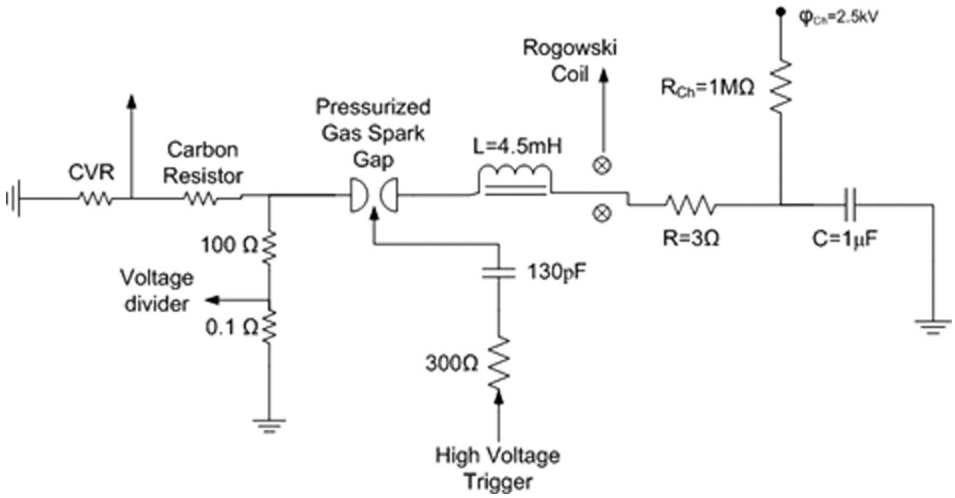

FIG. 7. Electrical circuit used for current supply through the low-inductance carbon resistor.

the temperature of the copper atoms is close to the boiling temperature ($T_{cu} \sim 3000$ K)of copper. This value of pressure is significantly smaller than the initial pressure at the outer surface of the tube. However, the tube implosion leads to an adiabatic increase in the inner pressure as $P/P_{0cu} \approx (V_0/V)^{\gamma} = (r_0/r)^{2\gamma}$, where $\gamma = 5/3$ and $r_0 \approx 0.4$ mm is the initial radius of the cavity. For $(r_0/r) \approx 2.5$, the pressure inside the cavity reaches the pressure value $P_1 \approx 10^{10}$Pa, and the temperature of the copper gas becomes $T_{cu} \approx 10^4$K. One can estimate that these parameters are reached during the time interval at time $\Delta t \sim 0.4 \times 10^{-6}$s with respect to the time when the primary converging SW reaches the outer surface of the tube. According to the results of numerical simulations, at that time, the pressure at the water-wall boundary decreases almost three times, i.e., $P_1 \approx 3 \times 10^9$Pa. Thus, one obtains the difference in pressure that leads to the explosion of the tube in the experiment.

Finally, we also conducted experiments using measurements of the pressure in the vicinity of the implosion of the spherical SW obtained by means of the change in the resistance of the low-inductance carbon resistor (0.88 mm in diameter) placed in the equatorial plane, similarly to the case of optical fiber. The electric scheme that was used to supply a pulsed current with an amplitude up to 300 A and pulse duration of ~ 5 μs through the resistor ($R = 50$ Ω, 0.125 W) is shown in Fig. 7. The discharge current and voltage were measured by a Pierson transformer coil and Tektronix voltage divider, respectively. Here, let us note that the measurements of the current via the resistor can be disturbed by the main discharge current, which is used to explode the wire array by mutual inductance and capacitance coupling. To avoid these disturbances, which are rather difficult to account for, the measurements of the current via the resistor should be performed when the main discharge is terminated. On the other hand, the current in the resistor should reach a rather large amplitude at the time when the converging SW approaches its location. In the present experimental conditions, the explosion of the spherical wire array with a diameter of 40 mm meets these conditions. Namely, according to numerical simulations, the explosion of such an array should lead to the generation of a converging SW whose TOF is ~ 9 μs,[12] i.e., such an SW would approach the resistor when the main discharge current is almost zero (see Figs. 2 and 3). Prior to the generator shot with a wire array explosion, a calibration shot with only current discharge via the resistor was performed, and the obtained calibration waveforms of the voltage and current were compared with the waveforms obtained with the shot with a wire array explosion in order to calculate the change in the resistance of the resistor R.

A typical result of these shots is shown in Fig. 8(a), where one can see a change in the resistance of the resistor R. In addition, one can see that the time when an increase in the current due to the decrease in the resistance of the carbon resistor caused by the increased pressure at that location is obtained begins at ~ 9.8 μs with respect to the start of the discharge current through the wire array. This time delay is ~ 1 μs larger than the time delay obtained in experiments with light emission from fibers and the results of simulations,

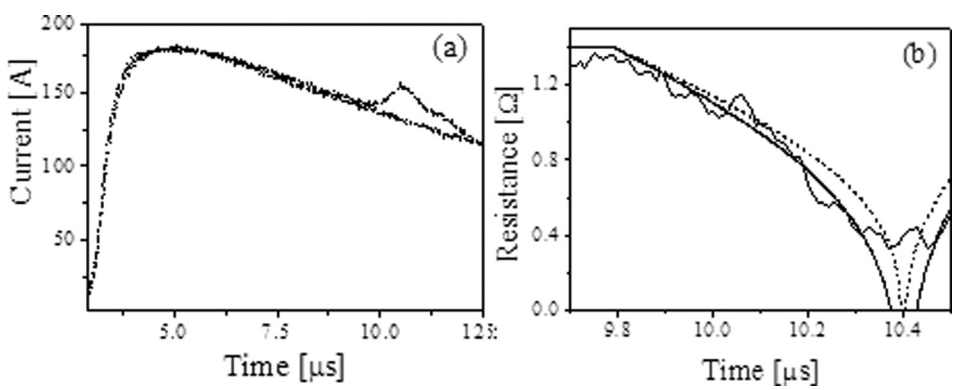

FIG. 8. (a) Typical waveform of the current through the carbon resistor without and with explosion of the spherical wire array; (b) Time-dependent change in the resistance of the carbon resistor together with the results of numerical simulations: the solid line is the results of simulations and the dashed line is the results of simulations with 2 times decreased pressure.

which give a time delay of ~8.8 μs. At the present, we have no explanation for the delay in the response of the carbon resistor and we can only mention that a similar phenomenon was obtained in earlier research.[24] These experimental data were compared with the results of numerical simulations in which the carbon resistor was considered as a sequence of many resistors R_{io} connected in series, experiencing the simulated pressure $P_i(t)$ evolution behind the front of the converging SW (see Fig. 8(b)). The time-dependent change in the resistance $\Delta R_i(t)$ of each resistor was calculated as[24] $P_i(t)[\mathrm{GPa}] = 13.54(\Delta R_i(t)/R_{io}) - 8.037$, where R_{0i} is the initial resistance. The results of these simulations can be compared with experimental results only up to $r = 0.44$ mm (~70 ns prior to the moment of the SW implosion), when the radius of the converging SW becomes smaller than the radius of the resistor and the assumption of many resistors connected in series is no longer valid. Here, let us note also that the calculated resistances were shifted artificially by ~1 μs to fit the experimental data. In order to test the sensitivity of this method, a two times smaller pressure than the simulated one was considered artificially. The results of these calculations are shown in Fig. 8(b). One can see that such a decrease in the pressure leads to a significantly worse fit with experimental data. Here, let us note that, if the convergence of the SW were not symmetrical, resulting in an even smaller pressure in the vicinity of the implosion, a larger difference between the simulated and experimental change in the resistance would be obtained.

In addition to those with the explosion of a 40 mm diameter wire array, experiments with explosions of spherical wire arrays having a diameter of 30 mm, 25 mm, and 20 mm and cylindrical wire arrays having a diameter of 15 mm and 12 mm and length of 40 mm were conducted, and their results were compared with the results of the 1D-HD simulations. In these experiments, the change in the resistance obtained also with a time delay of ~1 μs was compared with that expected according to the simulation result for the time delay of the SW arrival at the origin or axis of implosion and the results of other experiments using fiber light emission. The results of these experiments also showed a satisfactory agreement between the experimental and simulated values of the averaged changes in the resistance.

III. CONCLUSIONS

Experiments on underwater electrical wire array explosion showed that this approach can be used for the generation of converging SWs. The data obtained with light emission from the central part of the optical fiber, explosion of the copper tube, and changes in the resistor's resistance, placed in the equatorial plane of the array, together with the results of 1D-HD simulations, showed that this SW retains it uniformity along the major part of its convergence toward the origin of implosion. Thus, these results indicate that one can indeed obtain an extremely large pressure (10^{11} Pa and more) in the vicinity of the implosion origin in the case of a converging SW generated by the underwater electrical explosion of wire array.

ACKNOWLEDGMENTS

This research was supported by the Israeli Science Foundation grant No. 99/12.

[1]E. A. Martin, J. Appl. Phys. **31**, 255 (1960).
[2]A. V. Luchinskii, *Electrical Explosion of Wires* (Nauka, Moscow, 1989).
[3]S. V. Lebedev and A. I. Savvatimski, Sov. Phys. Usp. **27**, 749 (1984).
[4]A. C. Mitchel and W. J. Nellis, Rev. Sci. Instrum. **52**, 347 (1981).
[5]R. B. Spielman, C. Deeney, G. A. Chandler, M. R. Douglas, D. L. Fehl, M. K. Matzen, D. H. McDaniel, J. T. Nash, J. L. Porter, T. W. L. Sanford, J. F. Seaman, W. A. Stygar, K. W. Struve, S. P. Breeze, J. S. McGurn, J. A. Torres, D. M. Zagar, T. L. Gilliland, D. O. Jobe, J. L. McKenney, R. C. Mock, M. Vargas, T. Wagone, and D. L. Peterson, Phys. Plasmas **5**, 2105 (1998).
[6]P. M. Celliers, G. W. Collins, D. G. Hicks, M. Koenig, E. Henry, A. Benuzzi-Mounaix, D. Batani, D. K. Bradley, L. B. Da Silva, R. J. Wallace, S. J. Moon, J. H. Eggert, K. K. M. Lee, L. R. Benedetti, R. Jeanloz, I. Masclet, N. Dague, B. Marchet, M. Rabec Le Gloahec, Ch. Reverdin, J. Pasley, O. Willi, D. Neely, and C. Danson, Phys. Plasmas **11**, L41 (2004).
[7]K. Kolacek, V. Prukner, J. Schmidt, O. Frolov, and J. Straus, Laser Part. Beams **28**, 61 (2010).
[8]N. A. Tahir, Th. Stöhlker, A. Shutov, I. V. Lonosov, V. E. Fortov, M. French, N. Nettelmann, R. Redmer, A. R. Piriz, C. Deutch, Y. Zhao, H. Xu, G. Xiao, and W. Zhan, New J. Phys. **12**, 073022 (2010).
[9]T. Sasaki, Y. Yano, M. Nakajima, T. Kawamura, and K. Horioka, Laser Part. Beams **24**, 371 (2006).
[10]A. Grinenko, V. Tz. Gurovich, and Ya. E. Krasik, Phys. Plasmas **14**, 012701 (2007).
[11]S. Efimov, A. Fedotov, S. Gleizer, V. Tz. Gurovich, G. Bazalitski, and Ya. E. Krasik, Phys. Plasmas **15**, 112703 (2008).
[12]O. Antonov, S. Efimov, D. Yanuka, M. Kozlov, V. Tz. Gurovich, and Ya. E. Krasik, Appl. Phys. Lett. **102**, 124104 (2013).
[13]"Sesame: The Los Alamos National Laboratory equation-of-state database," edited by S. P. Lyon and J. D. Johnson, Los Alamos National Laboratory, Report No. LA-UR-92-3407 1992.
[14]A. Grinenko, S. Efimov, A. Fedotov, Ya. E. Krasik, and I. Schnitzer, J. Appl. Phys. **100**, 113509 (2006).
[15]S. Efimov, V. Tz. Gurovich, G. Bazalitski, A. Fedotov, and Ya. E. Krasik, J. Appl. Phys. **106**, 073308 (2009).
[16]M. Kozlov, V. Tz. Gurovich, and Ya. E. Krasik, Phys. Plasmas **20**, 112701 (2013).
[17]G. B. Whitham, *Linear and Nonlinear Waves* (Wiley, New York, 1974).
[18]Ya. E. Krasik, A. Grinenko, A. Sayapin, S. Efimov, A. Fedotov, V. Tz. Gurovich, and V. I. Oreshkin, IEEE Trans. Plasma Sci. **36**, 423 (2008).
[19]Ya. E. Krasik, A. Fedotov, D. Sheftman, S. Efimov, A. Sayapin, V. Tz. Gurovich, D. Veksler, G. Bazalitski, S. Gleizer, A. Grinenko, and V. I. Oreshkin, Plasma Sources Sci. Technol. **19**, 034020 (2010).
[20]O. Antonov, L. Gilburd, S. Efimov, G. Bazalitski, V. Tz. Gurovich, and Ya. E. Krasik, Phys. Plasmas **19**, 102702 (2012).
[21]A. Grinenko, A. Sayapin, V. Tz. Gurovich, S. Efimov, J. Felsteiner, and Ya. E. Krasik, J. Appl. Phys. **97**, 023303 (2005).
[22]Ya. B. Zel'dovich and Yu. P. Raizer, *Shock Waves and High-Temperature Hydrodynamic Phenomena* (Academic, New York, 1966).
[23]G. I. Pokrovskii, *Vzryv* (Izdatel'stvo "Nedra", Moscow, 1964) (in Russian).
[24]R. A. Lucht and J. A. Charest, AIP Conf. Proc. **370**(1), 1041–1044 (1996).